RESEARCH PAPER

DEVELOPMENT AND CHARACTERIZATION OF CHONDROITIN SULFATE NANOGEL FOR TOPICAL DELIVERY IN OSTEOARTHRITIS MANAGEMENT

Gaddam Mallikarjuna[1], K.E. Sailaja[2]*A. Mounika[3]

[1]Student, Department of Pharmaceutics, JNTUA–Oil Technological & Pharmaceutical Research Institute, Anantapur, Andhra Pradesh, India
[2]Assistant Professor, Department of Pharmaceutics, JNTUA–OTPRI, Anantapur, Andhra Pradesh, India
[3]Assistant Professor, Department of Pharmacology, JNTUA–OTPRI, Anantapur, Andhra Pradesh, India

Corresponding Author:
K.E. Sailaja
Assistant Professor, Department of Pharmaceutics, JNTUA–OTPRI, Anantapur, Andhra Pradesh, India
Email: ID: charansailaja1995@gmail.com

ABSTRACT

Chondroitin sulfate (CS) is an established therapeutic agent for osteoarthritis (OA), but conventional oral formulations suffer from poor bioavailability, first-pass metabolism, and gastrointestinal side effects. Nanogels represent a promising strategy for topical delivery, combining the advantages of hydrogels (high water content, biocompatibility) and nanoparticles (sustained release, targeted delivery) to enhance percutaneous drug transport. This study aimed to develop, optimize by Central Composite Design (CCD), and characterize CS-loaded nanogels using Eudragit RS 100 and Carbopol P 934 as polymer matrix components. Nine formulations (F1–F9) were prepared by the emulsion solvent diffusion method. The CCD optimized Eudragit RS 100 (0.358–0.641% w/v) and Carbopol P 934 (0.396–1.103% w/v) concentrations with entrapment efficiency (EE) and cumulative drug release (%CDR) as responses. Formulations were characterized for pH, viscosity, spreadability, drug content, EE, particle size, polydispersity index (PDI), and zeta potential. In vitro drug release was studied over 12 h using a Franz diffusion cell (phosphate buffer pH 6.8, 37°C). Release kinetics were modelled using zero-order, first-order, Higuchi, Hixson–Crowell, and Korsmeyer–Peppas equations. Accelerated stability testing followed ICH Q1A(R2) guidelines (40 ± 2°C/75 ± 5% RH, 90 days). All formulations showed acceptable physicochemical profiles (pH 5.4–5.7; viscosity 10,256–18,370 cps; drug content 71.10–92.43%). Optimised formulation F6 (Eudragit RS 100: 0.641%, Carbopol P 934: 0.75%) achieved EE 95.6%, %CDR 87.26% at 12 h, particle size 225.6 ± 0.5 nm, PDI 0.271 ± 0.02, and zeta potential −27.6 ± 0.22 mV. Drug release followed Higuchi kinetics (R^2 = 0.9946) with Korsmeyer–Peppas n = 1.2047, indicating super case II transport. ANOVA confirmed Eudragit RS 100 as the dominant factor for EE (F = 70.59, p = 0.0035) and %CDR (F = 73.16, p = 0.0034). Stability parameters remained within acceptance limits over 90 days. The CS nanogel F6 demonstrated superior physicochemical characteristics, controlled sustained release, and robust stability, validating its potential as an effective topical delivery platform for osteoarthritis management.

Keywords: Chondroitin sulfate; Nanogel; Eudragit RS 100; Carbopol P 934; Osteoarthritis; Sustained release; Central Composite Design; Topical drug delivery.
How to cite this article*:* Mallikarjuna G, Sailaja KE, Mounika A. Development and Characterization of Chondroitin Sulfate Nanogel for Topical Delivery in Osteoarthritis Management. Int J Drug Deliv Technol. 2026;16(62s): 1215-1229. DOI: 10.25258/ijddt.16.62s.129
Source of support: Nil.
Conflict of interest: Nil.

**Author for Correspondence:* charansailaja1995@gmail.com

INTRODUCTION

Osteoarthritis (OA) is the most prevalent degenerative joint disease globally, estimated to affect approximately 237 million individuals (3.3% of the world population) [4,5]. It is characterised by progressive articular cartilage degradation, subchondral bone remodelling, osteophyte formation, and synovial membrane inflammation, resulting in chronic pain, stiffness, reduced mobility, and significant disability [6,7]. Despite decades of research, no approved disease-modifying OA drug (DMOAD) is available in most markets, and current pharmacotherapy remains largely symptomatic. This underscores the clinical need for novel drug delivery strategies that enable sustained local drug concentrations with minimal systemic exposure.

Chondroitin sulfate (CS) is a naturally occurring sulfated glycosaminoglycan (GAG) constituting a key structural and functional component of the extracellular matrix (ECM) of articular cartilage [8]. Pharmacologically, CS reduces joint inflammation by inhibiting pro-inflammatory cytokines (IL-1beta, TNF-alpha) and matrix metalloproteinases (MMPs), while promoting proteoglycan and hyaluronic acid synthesis actions that collectively attenuate cartilage catabolism and support chondrocyte viability [9]. Despite these properties, oral CS formulations exhibit erratic bioavailability (10–24%) due to extensive first-pass hepatic metabolism, gastrointestinal intolerance at therapeutic doses, and prolonged latency to clinical effect [1,3]. Topical delivery is an attractive alternative, enabling direct delivery to periarticular tissues while bypassing systemic routes [2].

The principal barrier to topical drug absorption is the stratum corneum, who's ordered intercellular lipid lamellae restrict penetration of most macromolecules. Nanotechnology-based platforms in particular, nanogels have emerged as highly effective strategies for overcoming this barrier [26]. Nanogels are three-dimensional, crosslinked polymeric hydrogel networks at the nanoscale that integrate the attributes of both hydrogels (high water content, flexibility, biocompatibility, tunable mechanical properties) and nanoparticles (prolonged drug residence, passive targeting, large surface area-to-volume ratio) [24,25]. Nanosized particles can penetrate skin via follicular, transcellular, and intercellular routes, delivering drug directly to target tissues with minimal systemic uptake [27].

Eudragit RS 100 is an ammonio methacrylate copolymer with limited water permeability and robust film-forming capacity, enabling controlled drug release from polymer matrices. Carbopol P 934 is a crosslinked polyacrylic acid derivative widely used as a topical gelling agent owing to its mucoadhesive properties, viscoelastic behaviour, and concentration-dependent rheology. The rational combination of these polymers in a nanogel matrix offers independent control over encapsulation efficiency, release kinetics, and bioadhesion.

Response Surface Methodology (RSM) particularly Central Composite Design (CCD) is a validated statistical approach that models the formulation design space efficiently, quantifies linear and non-linear variable interactions, and identifies optimal operating conditions with fewer experiments than full factorial designs [35,36].

The present study reports the systematic development, CCD-based optimisation, and in vitro characterisation of CS-loaded nanogels for topical OA management. We hypothesised that by systematically varying Eudragit RS 100 and Carbopol P 934 concentrations, a nanogel formulation with superior EE, controlled %CDR, nanosized particles, and long-term stability could be achieved.

MATERIALS AND METHODS:

2.1 Materials

Chondroitin sulfate was obtained as a gift sample from Aurobindo Pharma Ltd. (Hyderabad, India). Eudragit RS 100 was procured from Evonik Industries AG (Darmstadt, Germany). Carbopol P 934 was supplied by Lubrizol Advanced Materials Inc. Tween 80, propylene glycol, and acetone (analytical grade) were sourced from S.D. Fine Chemicals Ltd. (Mumbai, India). Potassium dihydrogen phosphate and sodium hydroxide for buffer preparation were of analytical grade. All other chemicals were used as received without further purification.

2.2 Preformulation Studies

2.2.1 Organoleptic Properties and Solubility

Physical appearance, colour, odour, and texture of CS were recorded. Solubility was assessed in distilled water, phosphate buffer pH 6.8, ethanol, and acetone at 25 ± 1°C using the shake-flask saturation method.

2.2.2 Melting Point

The melting point of CS was determined in triplicate using an open-capillary melting point apparatus and compared with the reference standard range (245–250°C).

2.2.3 UV Spectrophotometric Analysis and Calibration Curve

A stock solution of CS (1000 µg/mL) in phosphate buffer pH 6.8 was prepared and diluted appropriately. The solution was scanned over 400–800 nm (Shimadzu UV-1800 spectrophotometer) to identify the wavelength of maximum absorbance (lambda-max). Working standard solutions (2–14 µg/mL) were prepared and absorbance recorded at lambda-max. Calibration data were fitted by linear regression (n = 3).

*Author for Correspondence: charansailaja1995@gmail.com

2.2.4 FTIR Compatibility Studies`

ATR-FTIR spectra of pure CS, Eudragit RS 100, Carbopol P 934, and their binary and ternary physical mixtures were recorded (PerkinElmer Spectrum Two, 4000–400 cm-1). Spectra were examined for shifts, broadening, or disappearances of characteristic peaks indicative of drug–excipient incompatibility.

2.2.5 Differential Scanning Calorimetry (DSC)

DSC thermograms of pure CS and its physical mixture with Eudragit RS 100 and Carbopol P 934 were obtained (Mettler Toledo DSC 3; nitrogen atmosphere; 10°C/min; 25–300°C; sample mass 5–10 mg). Changes in thermal transition temperatures or enthalpies were taken as indicative of incompatibility.

2.3 Experimental Design: Central Composite Design

A two-factor, five-level CCD (Design Expert Version 12, Stat-Ease Inc.) was employed to optimise the nanogel formulation. The independent variables were Factor A (Eudragit RS 100, % w/v) and Factor B (Carbopol P 934, % w/v) at five coded levels (-alpha, -1, 0, +1, +alpha). The dependent responses were EE (%) and %CDR at 12 h. Nine experimental runs (Table 1) were generated per the CCD matrix. Second-order polynomial equations were fitted to the response data and validated by ANOVA ($p < 0.05$). Contour and three-dimensional response surface plots were generated to visualise variable interactions.

Table 1. Composition of chondroitin sulfate nanogel formulations F1–F9 as per Central Composite Design

Ingredient	F1	F2	F3	F4	F5	F6	F7	F8	F9
Chondroitin sulfate (mg)	50	50	50	50	50	50	50	50	50
Eudragit RS 100 (% w/v)	0.40	0.60	0.40	0.60	0.358	0.641	0.50	0.50	0.50
Carbopol P 934 (% w/v)	0.50	0.50	1.00	1.00	0.75	0.75	0.396	1.103	0.75
Tween 80 (% w/v)	2	2	2	2	2	2	2	2	2
Propylene glycol (mL)	5	5	5	5	5	5	5	5	5
Acetone (mL)	10	10	10	10	10	10	10	10	10
Distilled water (mL)	q.s.	q.s.	q.s.	q.s.	q.s.	q.s.	q.s.	q.s.	q.s.

All formulations contained chondroitin sulfate 50 mg, Tween 80 2% w/v, propylene glycol 5 mL, and acetone 10 mL. q.s. = quantity sufficient with distilled water to 100 mL. n = 3 independent batches per formulation.

2.4 Preparation of Nanogels

CS (50 mg) and Eudragit RS 100 (as per Table 1) were dissolved in acetone to form the organic phase. Carbopol P 934 (as per Table 1) and Tween 80 (2% w/v) were dispersed in distilled water (aqueous phase) under gentle stirring. The organic phase was added dropwise (syringe pump, 1 mL/min) to the aqueous phase under continuous magnetic stirring (1200 rpm, room temperature). The resulting nanodispersion was stirred for 4 h to allow complete organic solvent evaporation. Propylene glycol (5 mL) was added as a humectant and penetration enhancer. pH was adjusted to 5.6 ± 0.2 using 0.1 M NaOH or HCl. The nanogel was stored in sealed amber vials at room temperature until evaluation.

2.5 Physicochemical Characterisation

pH was determined by dispersing 1 g nanogel in 10 mL phosphate buffer pH 6.8 and measuring with a calibrated digital pH meter (Elico LI120, n = 3). Spreadability was determined by the parallel plate method (0.5 g nanogel; 500 g weight; 5 min; n = 3); spreadability (g·cm/s) = M × L / T. Viscosity was measured at 25°C using a Brookfield rotational viscometer (spindle L4, 12 rpm; n = 3; results in centipoise). Drug content was quantified spectrophotometrically at lambda-max 651 nm after dissolving nanogel equivalent to 50 mg CS in phosphate buffer pH 6.8 (n = 3). Entrapment efficiency (EE) was calculated after centrifugation (15,000 rpm, 30 min): EE (%) = [(Total drug – Free drug in supernatant) / Total drug] × 100 (n = 3).

2.6 Particle Size, PDI, and Zeta Potential

Dynamic light scattering (Malvern Zetasizer Nano ZS; 25°C; 173-degree backscatter geometry) was used to

measure particle size, PDI, and zeta potential. Samples were diluted 1:100 (v/v) with deionized water. Results expressed as mean ± SD (n = 3).

2.7 In Vitro Drug Release Study

Franz diffusion cells (effective diffusion area 3.14 cm²; receptor compartment volume 15 mL) fitted with cellophane membrane (MWCO 12,000–14,000 Da) were used. Receptor medium: phosphate buffer pH 6.8 at 37 ± 0.5°C with 50 rpm continuous stirring. Donor compartment contained nanogel equivalent to 50 mg CS. Aliquots (1 mL) were withdrawn at 1, 2, 3, 4, 5, 6, 8, 10, and 12 h and replaced immediately with equal volumes of fresh buffer. Absorbance was measured at 651 nm and %CDR calculated from the calibration equation. Data were fitted to zero-order, first-order, Higuchi, Hixson–Crowell, and Korsmeyer–Peppas kinetic models (n = 3).

2.8 Accelerated Stability Studies

The optimised formulation (F6) was subjected to accelerated stability testing at 40 ± 2°C/75 ± 5% RH for 90 days (ICH Q1A[R2]). Samples were evaluated at days 0, 30, 60, and 90 for appearance, pH, viscosity, EE, and %CDR (n = 3).

2.9 Statistical Analysis

All data are expressed as mean ± SD (n = 3). CCD analysis and ANOVA were performed using Design Expert Version 12 (Stat-Ease Inc., Minneapolis, MN, USA). Statistical significance was set at $p < 0.05$.

RESULTS

3.1 Preformulation Studies

3.1.1 Organoleptic Properties and Solubility

Chondroitin sulfate appeared as a white to off-white, odourless, hygroscopic powder with a slightly acidic taste. Solubility studies confirmed that CS is freely soluble in water and phosphate buffer pH 6.8, but insoluble in ethanol and acetone. This profile informed the selection of a binary organic/aqueous solvent system for the emulsion solvent diffusion preparation method.

3.1.2 Melting Point

The melting point was determined to be 245.2°C (range: 244.8–245.6°C across three determinations), consistent with the reference standard range of 245–250°C, confirming identity and purity of the drug sample.

3.1.3 UV Spectrophotometric Analysis and Calibration Curve

CS in phosphate buffer pH 6.8 exhibited maximum absorbance at lambda-max = 651 nm. The calibration curve (2–14 µg/mL) was linear with regression equation: Absorbance = 0.0287 × C + 0.0012 (R^2 = 0.9997), confirming strict Beer–Lambert compliance across the analytical range (Figure 2).

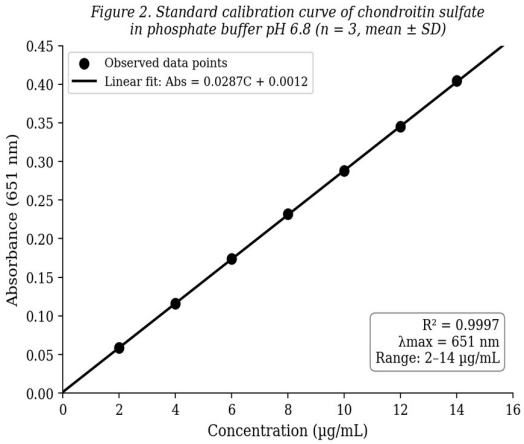

Figure 2. (A) UV absorption spectrum of chondroitin sulfate in phosphate buffer pH 6.8 showing lambda-max at 651 nm. (B) Standard calibration curve (2–14 µg/mL; n = 3). Regression equation: Abs = 0.0287C + 0.0012, R^2 = 0.9997.

3.1.4 FTIR Compatibility Studies

The FTIR spectrum of pure CS (Figure 3A) showed characteristic absorption bands: broad O–H stretch (3400 cm-1), C–H stretch (2930 cm-1), carboxylate C=O stretch (1620 cm-1), sulfate S=O stretch (1230 cm-1), and C–O–S bending (850 cm-1). These bands are consistent with the established CS structure. In the ternary physical mixture spectrum (Figure 3B), all principal CS peaks were retained at their original positions without significant shifts, broadening, or new bands. The appearance of an additional peak at 1730 cm-1 (ester C=O of Eudragit RS 100) was noted but did not interfere with CS peaks. These findings confirm the absence of drug–excipient chemical interaction.

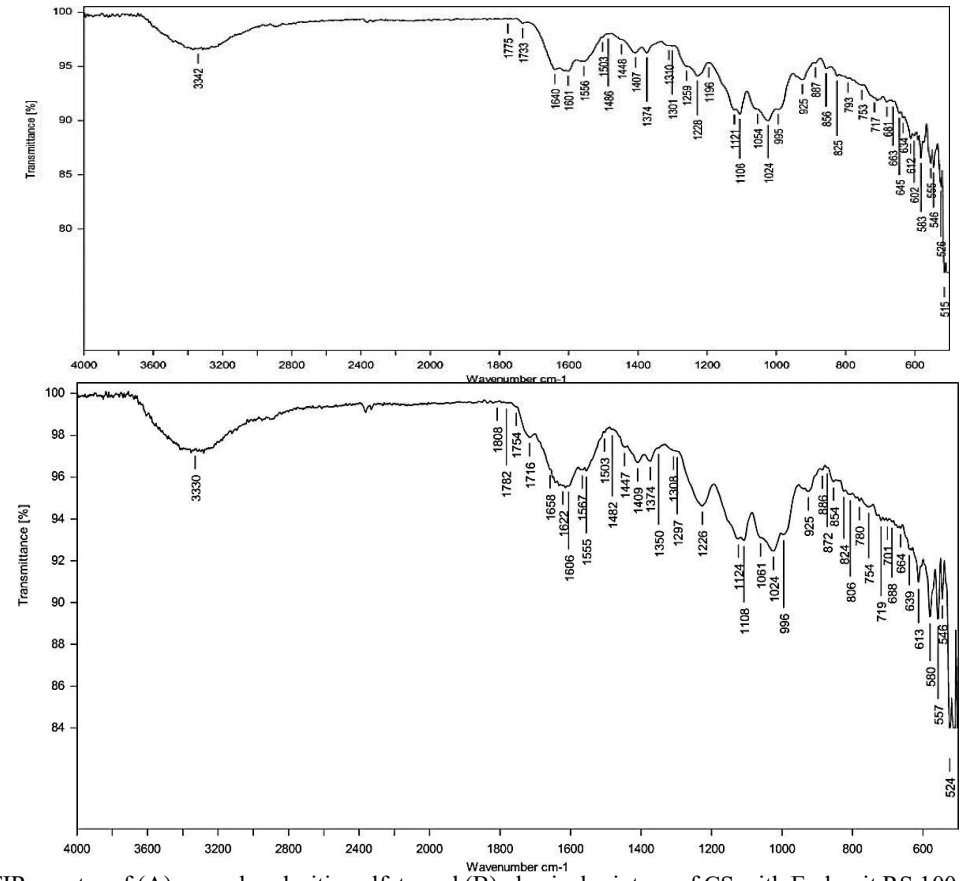

Figure 3. FTIR spectra of (A) pure chondroitin sulfate and (B) physical mixture of CS with Eudragit RS 100 and Carbopol P 934. Principal CS peaks (O–H: 3342 cm-1, C=O: 1640 cm-1, S=O: 1228 cm-1, C–O–S: 1054 cm-1) are retained in the mixture without significant shift, confirming drug–excipient compatibility

3.1.5 DSC Analysis

The DSC thermogram of pure CS (Figure 4A) exhibited a sharp endothermic peak at 245.2°C corresponding to melting/decomposition. In the physical mixture (Figure 4B), the CS endotherm was retained at the same temperature without significant change in onset, peak maximum, or enthalpy, confirming thermal compatibility between CS and both polymers. No new exothermic events were observed.

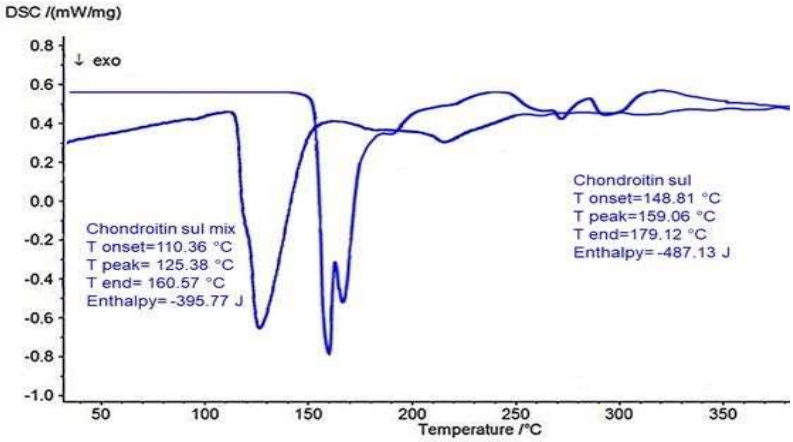

Figure 3. FTIR spectra of (A) pure chondroitin sulfate and (B) physical mixture of CS with Eudragit RS 100 and Carbopol P 934. Principal CS peaks (O–H: 3342 cm-1, C=O: 1640 cm-1, S=O: 1228 cm-1, C–O–S: 1054 cm-1) are retained in the mixture without significant shift, confirming drug–excipient compatibility.

3.2 Physicochemical Characterisation of Nanogels

3.2.1 Physical Appearance

All nine nanogel formulations were opaque, translucent gels exhibiting satisfactory to excellent homogeneity without phase separation or visible particle aggregation upon visual and tactile inspection. Formulations with higher polymer concentrations (F2, F4, F6, F8, F9) displayed excellent consistency, while those with lower polymer levels (F1, F3, F5, F7) were of satisfactory consistency — attributable to the lower gel network density at these concentrations.

3.2.2 pH, Spreadability, Viscosity, Drug Content, and EE

Results are presented in Table 2. pH values ranged from 5.4 ± 0.06 (F1, F5) to 5.7 ± 0.08 (F2, F8), within the skin-compatible range (4.5–7.0), minimising risk of dermal irritation during repeated application. Viscosity ranged from 10,256 ± 0.06 cps (F1) to 18,370 ± 0.05 cps (F6), increasing with polymer concentration and within the target range for topical application. Spreadability inversely correlated with viscosity. Drug content was acceptable in all formulations (71.10–92.43%), with F6 achieving the highest value (92.43 ± 0.08%). EE ranged from 75.0 ± 0.05% (F1) to 95.6 ± 0.08% (F6), with a clear positive correlation with Eudragit RS 100 concentration (Figure 5).

Figure 5. Entrapment efficiency (%) of CS nanogel formulations F1–F9 (mean ± SD, n = 3; F6 highlighted)

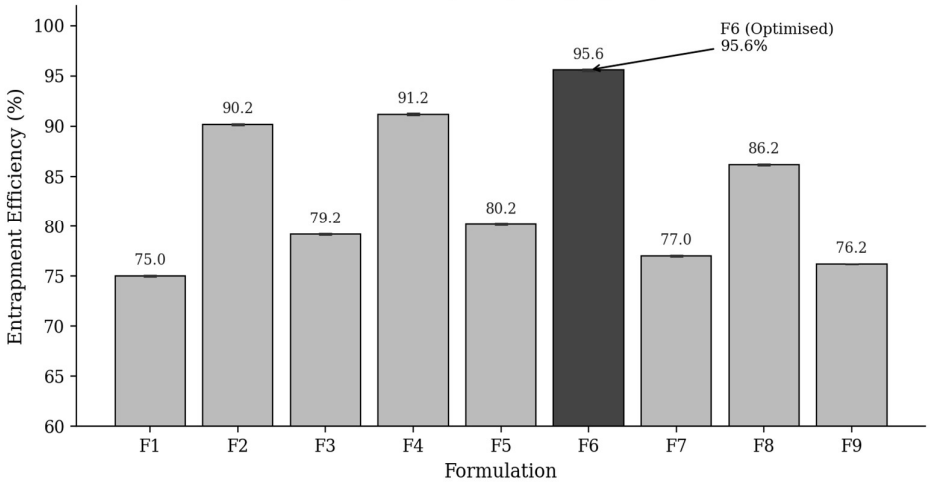

Figure 5. Entrapment efficiency (%) of chondroitin sulfate nanogel formulations F1–F9 (mean ± SD, n = 3; F6 shown in dark fill). F6 achieved the highest EE (95.6%), reflecting optimal polymer matrix density for drug encapsulation

Table 2. Physicochemical characterisation of chondroitin sulfate nanogel formulations F1–F9

Formulation	pH	Spreadability (g·cm/s)	Viscosity (cps)	Drug Content (%)	EE (%)
F1	5.4±0.06	13.21±0.04	10,256±0.06	72.40±0.04	75.0±0.05
F2	5.7±0.08	11.23±0.05	17,890±0.08	89.20±0.06	90.2±0.07
F3	5.5±0.04	12.52±0.03	12,450±0.04	73.10±0.03	79.2±0.04
F4	5.6±0.07	10.56±0.07	18,120±0.07	91.10±0.07	91.2±0.08
F5	5.4±0.05	13.80±0.06	11,230±0.05	71.10±0.05	80.2±0.06
F6	5.6±0.13	9.85±0.08	18,370±0.05	92.43±0.08	95.6±0.08
F7	5.5±0.09	12.10±0.04	13,560±0.06	74.80±0.04	77.0±0.05
F8	5.7±0.06	10.23±0.05	17,340±0.07	88.60±0.07	86.2±0.06
F9	5.6±0.04	11.46±0.03	15,890±0.08	81.20±0.05	76.2±0.03

3.3 In Vitro Drug Release

Cumulative drug release profiles over 12 h are shown in Table 3 and Figure 6. All formulations displayed progressive, sustained release throughout the study period. Formulation F6 achieved the highest %CDR (87.26% at 12 h), followed by F4 (73.34%), F8 (69.64%), and F2 (65.01%). Drug release was concentration-dependent: higher Eudragit RS 100 concentrations consistently produced greater %CDR, while higher Carbopol P 934 concentrations increased gel network viscosity and partially retarded release. No burst release was observed in any formulation.

Table 3. Cumulative percentage drug release (%CDR) of chondroitin sulfate nanogel formulations F1–F9 over 12 hours

Time (h)	F1	F2	F3	F4	F5	F6	F7	F8	F9
1	14.62	9.61	17.01	18.48	13.52	17.49	14.54	15.50	11.45
2	15.78	14.01	20.48	26.14	17.74	26.18	18.74	21.07	14.51
3	16.78	18.57	22.24	30.97	22.02	31.44	22.96	26.38	17.52
4	19.47	24.62	31.12	36.95	25.52	37.68	27.20	31.94	21.27
5	22.03	38.27	35.44	41.44	28.49	43.30	31.00	37.24	24.99
6	24.08	47.53	38.94	46.02	31.38	50.28	34.56	42.44	27.68
8	27.44	59.46	40.68	53.63	34.21	57.80	38.46	49.50	30.95
10	34.53	61.35	43.44	61.68	38.46	65.67	42.51	56.56	33.87
12	44.35	65.01	50.74	73.34	48.06	87.26	55.44	69.64	43.69

Values represent mean %CDR (n = 3). Dissolution medium: phosphate buffer pH 6.8, 37 ± 0.5°C, Franz diffusion cell with cellophane membrane (MWCO 12,000–14,000 Da).

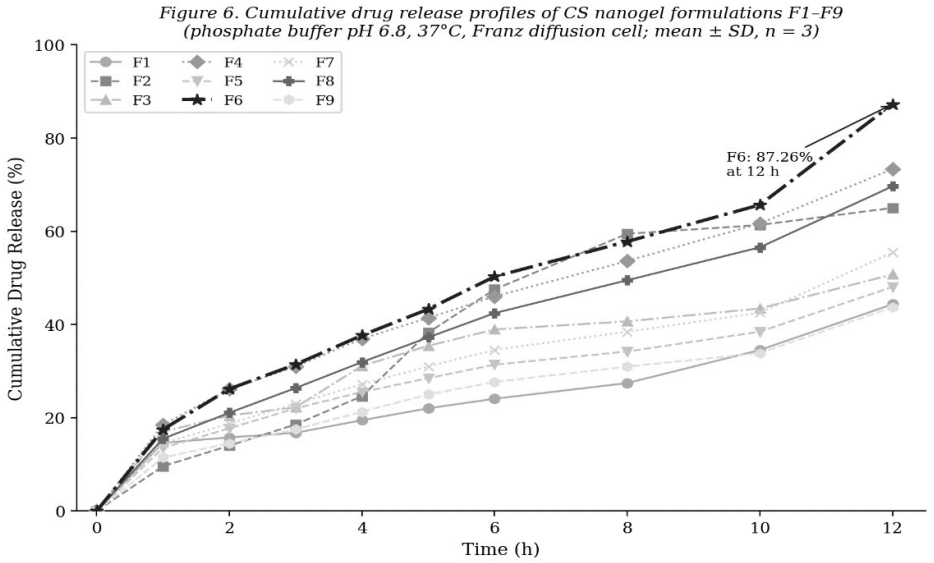

Figure 6. Comparative cumulative drug release profiles of CS nanogel formulations F1–F9 (phosphate buffer pH 6.8, 37 ± 0.5°C, Franz diffusion cell). F6 demonstrated the highest sustained release (87.26% at 12 h). Data represent mean ± SD (n = 3).

3.4 Drug Release Kinetics

Regression coefficients for all kinetic models are presented in Table 4. The Higuchi model provided the best fit across all formulations (R^2 range: 0.9256–0.9959), indicating a diffusion-controlled release mechanism from the polymer matrix. For F6, the Higuchi R^2 was 0.9946 — the highest among all formulations. The zero-order R^2 for F6 was 0.9507, consistent with a concentration-independent release profile. Korsmeyer–Peppas analysis revealed n values exceeding 1.0 for formulations F2, F4, F6, and F8 (maximum n = 1.2781 for F2; F6 n = 1.2047), indicating super case II transport in which polymer chain relaxation and matrix erosion drive drug release alongside diffusion (Figure 7).

Table 4. Regression coefficient (R^2) values and Korsmeyer–Peppas n value for CS nanogel formulations F1–F9

Formulation	Zero Order (R^2)	First Order (R^2)	Higuchi (R^2)	Hixson–Crowell (R^2)	Korsmeyer–Peppas (R^2)	n value
F1	0.8827	0.9934	0.9420	0.9632	0.6295	0.9357

F2	0.9440	0.8559	0.9256	0.9417	0.7899	1.2781
F3	0.8629	0.8586	0.9789	0.9234	0.5782	0.9773
F4	0.9433	0.8846	0.9959	0.9734	0.6177	1.1080
F5	0.9330	0.8898	0.9921	0.9837	0.6073	0.9691
F6	0.9507	0.8610	0.9946	0.9675	0.6632	1.2047
F7	0.9433	0.8890	0.9804	0.9820	0.5935	0.9670
F8	0.9580	0.9114	0.9829	0.9862	0.8873	1.1014
F9	0.9440	0.9282	0.9559	0.9700	0.6295	0.9357

The Higuchi model provided the highest R² values across all formulations, confirming diffusion-controlled release. Formulations F2, F4, F6, and F8 with n > 1.0 indicate super case II (erosion-mediated) transport.

Figure 7. Drug release kinetics of CS nanogel formulations.
(A) Higuchi model; (B) Korsmeyer–Peppas model (n > 1.0 indicates super case II transport)

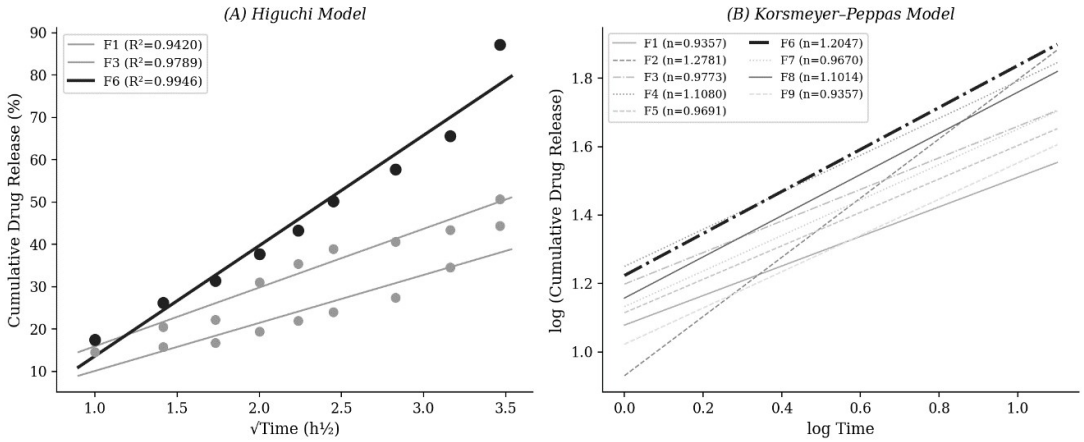

Figure 7. Drug release kinetics of CS nanogel formulations. (A) Higuchi model (cumulative %CDR vs. square root of time); (B) Korsmeyer–Peppas model (log %CDR vs. log time). F6 Higuchi R² = 0.9946; n = 1.2047, confirming erosion-mediated sustained release.

3.5 Central Composite Design Optimisation

3.5.1 Effect of Variables on Entrapment Efficiency

The CCD quadratic polynomial equation for EE was: EE (%) = 76.2 + 6.122A + 2.276B – 0.8AB + 5.638A² + 2.488B². The ANOVA (Table 5) confirmed model significance (F = 20.82, p = 0.0155; adjusted R² = 0.9253). Factor A (Eudragit RS 100) was the primary determinant of EE (F = 70.59, p = 0.0035), reflecting its dominant role in forming the drug-entrapping polymer network. Response surface and contour plots (Figure 8) showed that EE increased steeply with Eudragit RS 100 concentration, with Carbopol P 934 providing a secondary optimising effect at mid-range concentrations.

Table 5. ANOVA for the CCD quadratic model — Response 1: Entrapment Efficiency (EE, %)

Source	Sum of Squares	df	Mean Square	F-value	p-value	Significance
Model	442.25	5	88.45	20.82	0.0155	Significant
A – Eudragit RS 100	299.87	1	299.87	70.59	0.0035	
B – Carbopol P 934	41.45	1	41.45	9.76	0.0523	
AB (Interaction)	2.56	1	2.56	0.60	0.4942	
A²	92.45	1	92.45	21.76	0.0186	
B²	18.00	1	18.00	4.24	0.1317	
Residual	12.74	3	4.25	—	—	
Cor Total	455.00	8	—	—	—	

SS = sum of squares; df = degrees of freedom; MS = mean square. Model F-value 20.82, p = 0.0155. Factor A (Eudragit RS 100) was the dominant predictor (F = 70.59, p = 0.0035).

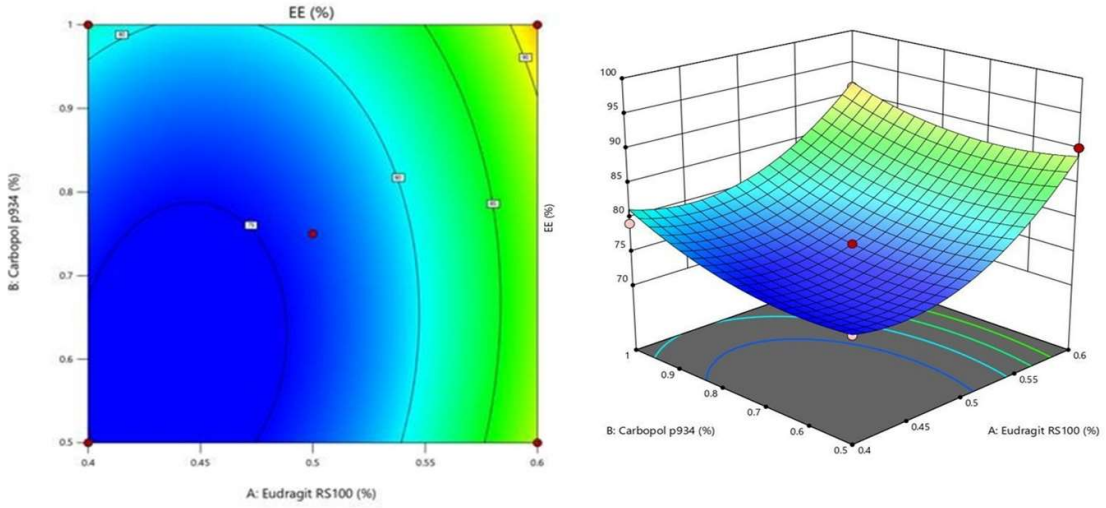

Figure 8. CCD response surface plots for entrapment efficiency (EE%). (A) 2D contour plot showing EE increasing toward higher Eudragit RS 100 concentrations. (B) 3D response surface confirming the dominant effect of Factor A (Eudragit RS 100) on EE. Maximum predicted EE achieved at upper Factor A boundary with moderate Factor B.

3.5.2 Effect of Variables on Cumulative Drug Release

The polynomial equation for %CDR was: CDR (%) = 33.6 + 12.858A + 4.038B – 2.425AB + 12.356A² + 6.956B². ANOVA (Table 6) confirmed model significance (F = 21.29, p = 0.0150; adjusted R^2 = 0.9269). Eudragit RS 100 was again the primary predictor (F = 73.16, p = 0.0034). The quadratic term for Factor A (F = 24.57, p = 0.0158) indicated a non-linear concentration–response relationship. Surface plots (Figure 9) demonstrated maximum %CDR at high Eudragit RS 100 with moderate Carbopol P 934, as in formulation F6.

Table 6. ANOVA for the CCD quadratic model — Response 2: Cumulative Drug Release (%CDR at 12 h)

Source	Sum of Squares	df	Mean Square	F-value	p-value	Significance
Model	1924.82	5	384.96	21.29	0.0150	Significant
A – Eudragit RS 100	1322.68	1	1322.68	73.16	0.0034	
B – Carbopol P 934	130.45	1	130.45	7.22	0.0747	
AB (Interaction)	23.52	1	23.52	1.30	0.3368	
A²	444.15	1	444.15	24.57	0.0158	
B²	140.77	1	140.77	7.79	0.0684	
Residual	54.24	3	18.08	—	—	
Cor Total	1979.06	8	—	—	—	

Model F-value 21.29, p = 0.0150. Factor A (Eudragit RS 100) dominant (F = 73.16, p = 0.0034). SS = sum of squares; MS = mean square.

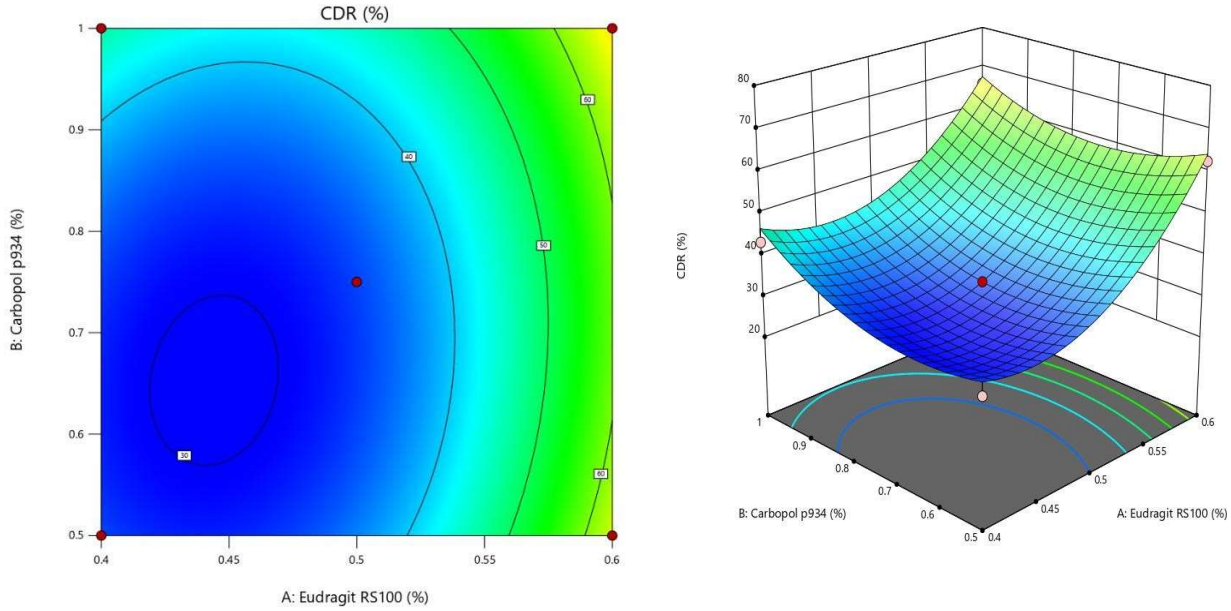

Figure 9. CCD response surface plots for cumulative drug release (%CDR at 12 h). (A) 2D contour plot showing %CDR increasing with Eudragit RS 100 concentration. (B) 3D response surface demonstrating the quadratic relationship between polymer concentrations and drug release. Maximum %CDR achieved at upper Factor A (Eudragit RS 100) boundary.

3.6 Particle Size, PDI, and Zeta Potential

Results are presented in Table 7. Particle sizes ranged from 225.6 ± 0.5 nm (F6) to 250.6 ± 0.5 nm (F4), within the optimal range for transdermal delivery. PDI values were consistently below 0.280 across all formulations (0.271–0.2750), confirming narrow, homogeneous size distributions — a critical attribute for reproducible topical performance. Zeta potential values ranged from −27.3 ± 0.20 mV (F4) to −29.4 ± 0.40 mV (F7). The high magnitude of negative zeta potential across all formulations reflects strong electrostatic repulsion between particles, ensuring colloidal stability (Figure 10).

Table 7. Particle size, polydispersity index (PDI), and zeta potential of CS nanogel formulations F1–F9

Formulation	Particle Size (nm)	PDI	Zeta Potential (mV)
F1	243.81 ± 0.8	0.274 ± 0.03	-27.9 ± 0.20
F2	249.53 ± 0.4	0.2715 ± 0.02	-28.5 ± 0.31
F3	225.70 ± 0.6	0.272 ± 0.03	-29.1 ± 0.40
F4	250.60 ± 0.5	0.2725 ± 0.02	-27.3 ± 0.20
F5	235.98 ± 0.7	0.273 ± 0.03	-28.8 ± 0.33
F6	225.60 ± 0.5	0.271 ± 0.02	-27.6 ± 0.22
F7	245.29 ± 0.4	0.2735 ± 0.03	-29.4 ± 0.40
F8	239.46 ± 0.5	0.275 ± 0.03	-28.0 ± 0.30
F9	228.60 ± 0.3	0.274 ± 0.03	-28.7 ± 0.31

Values expressed as mean ± SD (n = 3). PDI < 0.3 indicates a narrow size distribution. Negative zeta potential (|ZP| > 25 mV) confirms adequate colloidal stability against aggregation.

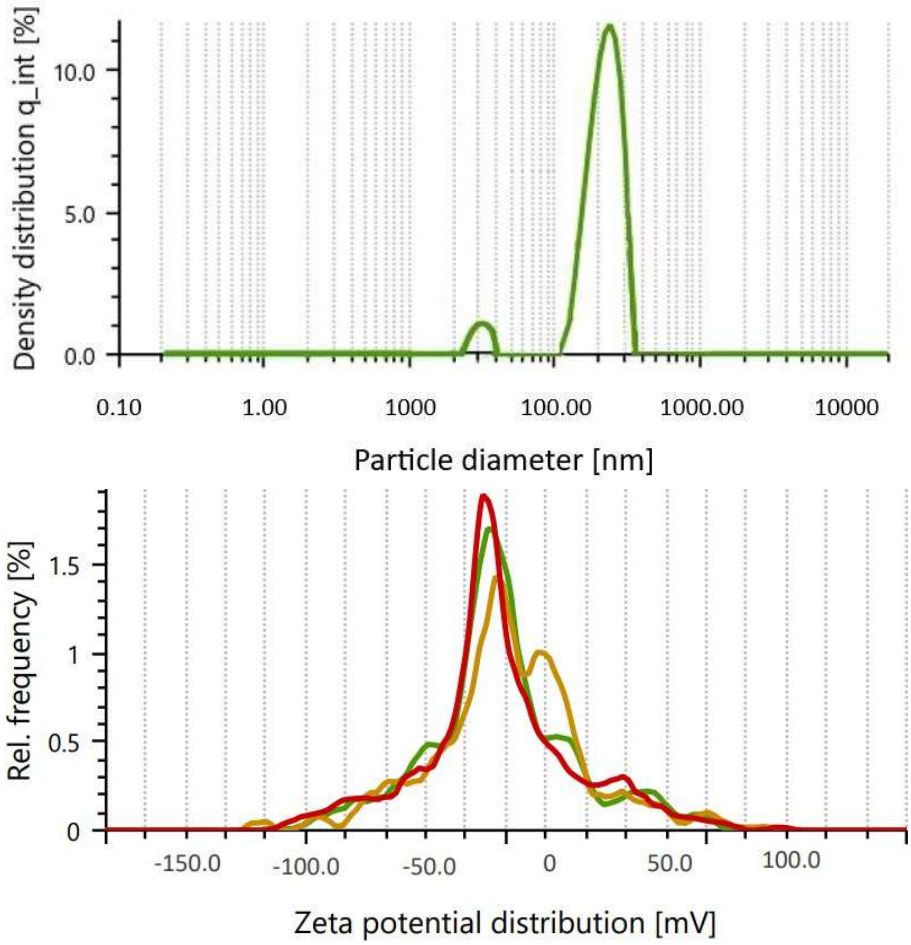

Figure 10. Dynamic light scattering characterisation of optimised formulation F6. (A) Particle size distribution profile (Malvern Zetasizer Nano ZS) showing the primary nanogel peak at 225.6 ± 0.5 nm with PDI 0.271 ± 0.02, confirming narrow size distribution. (B) Zeta potential distribution with mean −27.6 ± 0.22 mV across three runs (red, green, orange traces), confirming adequate colloidal stability. Data: mean ± SD (n = 3).

3.7 Accelerated Stability Studies

Stability data for the optimised formulation F6 over 90 days at 40 ± 2°C/75 ± 5% RH are presented in Table 8 and Figure 11. All parameters showed only minor, non-significant changes over the study period. Appearance remained consistently opaque throughout. pH decreased marginally from 5.60 ± 0.05 (day 0) to 5.45 ± 0.07 (day 90), remaining within the skin-compatible range. Viscosity decreased slightly (18,370 to 17,650 cps), attributable to polymer chain relaxation under thermal stress. EE declined from 95.6 ± 0.08% to 90.5 ± 0.06%, and %CDR reduced from 87.6 ± 0.07% to 83.7 ± 0.06% at day 90. These minor changes remained within predefined acceptance limits, confirming the robustness of the formulation.

Table 8. Accelerated stability data for optimised formulation F6 (40°C/75% RH, 90 days, ICH Q1A[R2])

Day	Appearance	pH	Viscosity (cps)	EE (%)	% CDR at 12 h
0	Opaque	5.60 ± 0.05	18,370 ± 0.05	95.6 ± 0.08	87.6 ± 0.07
30	Opaque	5.55 ± 0.08	18,120 ± 0.08	93.8 ± 0.07	86.2 ± 0.01
60	Opaque	5.50 ± 0.09	17,900 ± 0.07	92.1 ± 0.05	85.0 ± 0.05
90	Opaque	5.45 ± 0.07	17,650 ± 0.09	90.5 ± 0.06	83.7 ± 0.06

Values expressed as mean ± SD (n = 3). All changes over 90 days were within predefined acceptance limits, confirming formulation stability over the study period.

Figure 11. Stability profiles of optimised formulation F6 (40°C/75% RH, ICH Q1A[R2]). (A) Entrapment efficiency; (B) % CDR at 12 h; (C) Viscosity. Data: mean ± SD (n = 3).

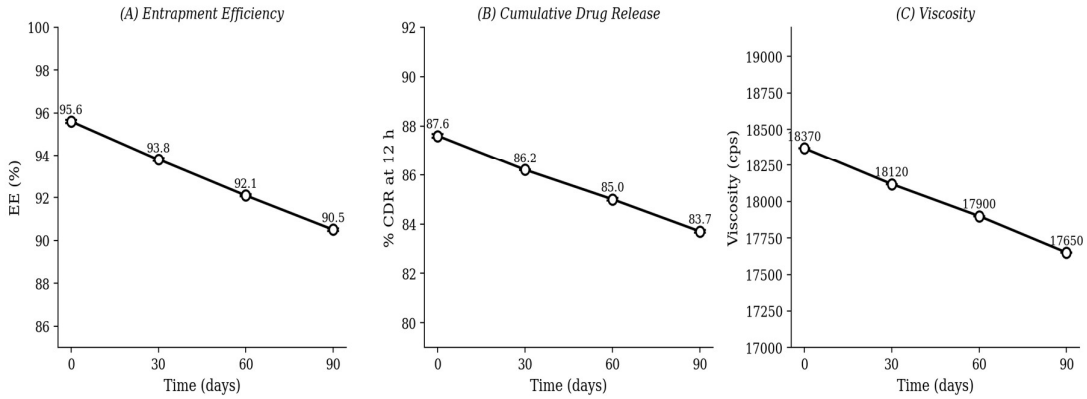

Figure 11. Stability profiles of optimised formulation F6 (40°C/75% RH, ICH Q1A[R2], 90 days). (A) Entrapment efficiency (%); (B) Cumulative drug release (%CDR at 12 h); (C) Viscosity (cps). All parameters remained within acceptance criteria. Data: mean ± SD (n = 3).

DISCUSSION:

The present investigation successfully demonstrated the feasibility of a CS-loaded nanogel as a topical delivery platform for osteoarthritis management. The emulsion solvent diffusion method provided a scalable, reproducible approach to fabricating stable nanodispersions without high-energy sonication or elevated temperature — attributes important for preserving the structural integrity of the sulfated polysaccharide CS [27,28].

Preformulation studies confirmed that CS is both chemically and thermally compatible with Eudragit RS 100 and Carbopol P 934 — a prerequisite for stable formulation development. The absence of new FTIR bands or significant spectral shifts in the physical mixture indicates no covalent drug–excipient interaction [29]. Retention of the CS melting endotherm in DSC thermograms at its characteristic temperature confirms that neither polymer altered the thermal behaviour or crystallinity of CS, consistent with findings reported by Saraogi et al. [36] and Alam et al. [37] for related nanogel systems.

All nanogel formulations exhibited pH values (5.4–5.7) and viscosity profiles (10,256–18,370 cps) suitable for topical application. The slightly acidic pH mirrors physiological skin surface pH (4.5–6.0), reducing the risk of irritation and maintaining skin barrier integrity during chronic OA management [1]. Viscosity values in the target range (10,000–20,000 cps) ensure adequate bioadhesion, film formation, and patient acceptability without impeding drug diffusion to the tissue interface [30].

The pronounced positive correlation between Eudragit RS 100 concentration and EE is consistent with the formation of a denser hydrophobic polymer network at higher concentrations, which more effectively entraps CS molecules and resists their partitioning into the external aqueous phase during preparation. Carbopol P 934 reinforces this entrapment by contributing a crosslinked, mucoadhesive polyacrylic acid network that physically restricts drug escape [33,34]. The superior EE of F6 (95.6%) aligns with findings of Alam et al. [37] and Avasatthi et al. [43], who demonstrated EE enhancement with increasing polymer matrix density in aceclofenac and methotrexate nanogel systems, respectively.

The progressive, sustained drug release profiles observed across all formulations are consistent with the design objective of a controlled-release topical system. The highest %CDR of F6 (87.26% at 12 h) can be attributed to the combined effect of its optimal Eudragit RS 100 concentration — which facilitates sufficient drug diffusivity through the matrix — and the moderate Carbopol P 934 content, which maintains gel network integrity without excessive viscosity that would otherwise retard membrane transport. The Higuchi model (R^2 = 0.9946 for F6) provides the best mathematical description of drug release, confirming square-root-of-time dependent diffusion from a homogeneous polymer matrix [35]. The Korsmeyer–Peppas n value of 1.2047 for F6 indicates super case II transport — a drug release mechanism governed by polymer chain relaxation and matrix erosion superimposed on Fickian diffusion. Similar transport mechanisms were reported for tenoxicam nanogels by Chopade et al. [41] and for methotrexate nanogels by Avasatthi et al. [43].

The CCD optimisation provided a rigorous, statistically validated characterisation of the formulation design space. The highly significant quadratic models for both EE and %CDR ($p < 0.05$) with adjusted R^2 values exceeding 0.92 confirm strong predictive capability and minimal lack-of-

fit. The statistical dominance of Factor A (Eudragit RS 100) over Factor B (Carbopol P 934) across both responses reflects the critical role of the primary film-forming polymer in determining encapsulation and release, consistent with Eudragit RS 100's known permeability-limiting properties in polymer matrices [36]. The significant quadratic term for Factor A in both models (EE: $F = 21.76$, $p = 0.0186$; %CDR: $F = 24.57$, $p = 0.0158$) indicates an optimal concentration window rather than a purely monotonic relationship, enabling precise identification of the optimal formulation.

Particle sizes in the range 225.6–250.6 nm are well-suited for transdermal delivery. Particles below 300 nm can permeate skin via appendageal routes (hair follicle openings, sweat gland ducts) and exploiting intercellular lipid discontinuities in the stratum corneum, enabling delivery of the drug to the deeper viable epidermis and dermis proximal to the target joint tissues [1,3]. PDI values below 0.280 confirm narrow, monodisperse size distributions — important for regulatory compliance and predictable pharmacokinetic behaviour. Negative zeta potentials (−27.3 to −29.4 mV) confirm adequate colloidal stability through electrostatic repulsion, preventing particle aggregation during storage. The negative surface charge of all nanogel formulations is attributable to the ionised carboxylate groups of Carbopol P 934 at formulation pH [24,25].

The accelerated stability data confirmed the physicochemical robustness of F6 over 90 days under ICH conditions. The minor reductions in EE (−5.1%) and %CDR (−3.9%) are consistent with partial polymer hydrolysis and water activity-driven network relaxation under high humidity stress — processes commonly reported for acrylic polymer-based nanogels [43,44]. The stability profile of F6 compares favourably with that of pravastatin nanogels [36] and chitosan-based nanogels [44], in which analogous stability trends were documented under equivalent ICH conditions.

Taken together, these results establish the CS nanogel as a compelling topical alternative to conventional oral CS administration, directly addressing the key limitations of oral formulations: poor and variable bioavailability, gastrointestinal intolerance, and high required doses. Limitations of this study include reliance on a synthetic cellophane membrane rather than biological tissue for drug release assessment, and the absence of in vivo validation. Future investigations should incorporate ex vivo permeation studies using full-thickness or dermatomed human skin, confocal laser scanning microscopy to visualise follicular and transdermal penetration pathways, and in vivo pharmacokinetic and pharmacodynamic evaluation in validated OA animal models. Skin safety profiling — including primary irritation, sensitisation, and repeated-dose dermal toxicity — will also be essential before clinical translation.

CONCLUSION:

A chondroitin sulfate nanogel was successfully formulated and optimised by the emulsion solvent diffusion method using a Central Composite Design. Eudragit RS 100 and Carbopol P 934 were identified as the critical formulation variables governing entrapment efficiency and cumulative drug release, with Eudragit RS 100 exerting the dominant effect on both responses. The optimised formulation F6 (Eudragit RS 100: 0.641% w/v, Carbopol P 934: 0.75% w/v) demonstrated superior performance: EE 95.6%, %CDR 87.26% at 12 h, particle size 225.6 ± 0.5 nm, PDI 0.271 ± 0.02, zeta potential −27.6 ± 0.22 mV, and a skin-compatible pH of 5.6 ± 0.13. Drug release followed the Higuchi model with super case II transport kinetics ($n = 1.2047$), confirming a sustained, erosion-mediated diffusion mechanism appropriate for OA therapy. Accelerated stability testing at 40°C/75% RH for 90 days confirmed formulation robustness within ICH acceptance criteria. These findings collectively validate the CS nanogel as a clinically promising platform for enhanced local drug delivery in osteoarthritis management, supporting its progression to in vivo pharmacokinetic and efficacy evaluation.

FUNDING: This research received no external funding. It was conducted as part of the M. Pharmacy research programme.

CONFLICTS OF INTEREST: The author declares no conflict of interest.

ACKNOWLEDGEMENT:
The authors sincerely thank the Department of Pharmaceutical Analysis, JNTUA–OTPRI College of Pharmaceutical Sciences, for providing the necessary facilities and support to carry out this research work.

REFERENCE

1. Singh Malik D, Mital N, Kaur G. Topical drug delivery systems: a patent review. Expert Opin Ther Pat. 2016;26(2):213–228.
2. Rawlings AV. Ethnic skin types: are there differences in skin structure and function? Int J Cosmet Sci. 2006;28(2):79–93.
3. Ng KW, Lau WM. Skin deep: the basics of human skin structure and drug penetration. In: Dragicevic N, Maibach HI, eds. Percutaneous Penetration Enhancers: Chemical Methods in Penetration Enhancement. Berlin: Springer; 2015:3–11.
4. Kahan A, Uebelhart D, De Vathaire F, Delmas PD, Reginster JY. Long-term effects of chondroitins 4 and 6 sulfate on knee osteoarthritis: the study on

osteoarthritis progression prevention. Arthritis Rheum. 2009;60(2):524–533.

5. National Institutes of Health. National Institute of Arthritis and Musculoskeletal and Skin Diseases. Handout on Health: Osteoarthritis. NIH Publication; 2001.
6. Sanchez-Adams J, Leddy HA, McNulty AL, O'Connor CJ, Guilak F. The mechanobiology of articular cartilage: bearing the burden of osteoarthritis. Curr Rheumatol Rep. 2014;16(10):451.
7. Maroudas AI. Balance between swelling pressure and collagen tension in normal and degenerate cartilage. Nature. 1976;260(5554):808–809.
8. Henrotin Y, Mathy M, Sanchez C, Lambert C. Chondroitin sulfate in the treatment of osteoarthritis: from in vitro studies to clinical recommendations. Ther Adv Musculoskelet Dis. 2010;2(6):335–348.
9. Volpi N, Schiller J, Stern R, Soltes L. Chondroitin sulfate: structure, role and pharmacological activity. Molecules. 2019;24(5):908.
10. Iacob S, Vasile C. Chondroitin sulfate as a valuable ingredient of biomaterials for tissue engineering: a review. Carbohydr Polym. 2021;273:118766.
11. Nasrollahzadeh M, Sajadi SM, Sajjadi M, Issaabadi Z. An introduction to nanotechnology. Interface Sci Technol. 2019;28:1–27.
12. Gharpure KM, Wu SY, Li C, Lopez-Berestein G, Sood AK. Nanotechnology: future of oncotherapy. Clin Cancer Res. 2015;21(14):3121–3130.
13. Hornyak GL, Moore JJ, Tibbals HF, Dutta J. Fundamentals of Nanotechnology. Boca Raton: CRC Press; 2018.
14. Rai M, dos Santos CA, eds. Nanotechnology Applied to Pharmaceutical Technology. Cham: Springer; 2017.
15. Sharma D, Sharma N, Pathak M, Agrawala PK, Basu M, Ojha H. Nanotechnology-based drug delivery systems: challenges and opportunities. In: Grumezescu AM, ed. Drug Targeting and Stimuli-Sensitive Drug Delivery Systems. Amsterdam: Elsevier; 2018:39–79.
16. Suttee A, Singh G, Yadav N, Barnwal RP, Singla N, Mishra V. A review on the status of nanotechnology in pharmaceutical sciences. Int J Drug Deliv Technol. 2019;9:98–103.
17. Prakash S, Karacor MB, Banerjee S. Surface modification in microsystems and nanosystems. Surf Sci Rep. 2009;64(7):233–254.
18. Ferraris C, Rimicci C, Garelli S, Ugazio E, Battaglia L. Nanosystems in cosmetic products. Pharmaceutics. 2021;13(9):1408.
19. Smith DM, Simon JK, Baker JR Jr. Applications of nanotechnology for immunology. Nat Rev Immunol. 2013;13(8):592–605.
20. DeLouise LA. Applications of nanotechnology in dermatology. J Invest Dermatol. 2012;132(3):964–975.
21. Napagoda M, Wijayaratne GB, Witharana S. Applications of nanotechnology in dermatology. In: Grumezescu AM, ed. Nanotechnology in Modern Medicine. Singapore: Springer Nature; 2022:135–168.
22. Saraceno R, Chiricozzi A, Gabellini M, Chimenti S. Emerging applications of nanomedicine in dermatology. Skin Res Technol. 2013;19(1):e13–e19.
23. Saraceno R, Chiricozzi A, Botti E, et al. Nanomedicine in dermatology: benefits and emerging applications. In: Patenting Nanomedicines. Berlin: Springer; 2012:383–399.
24. Vinogradov SV. Nanogels in the race for drug delivery. Nanomedicine (Lond). 2010;5(2):165–168.
25. Kabanov AV, Vinogradov SV. Nanogels as pharmaceutical carriers: finite networks of infinite capabilities. Angew Chem Int Ed Engl. 2009;48(30):5418–5429.
26. Zha L, Banik B, Alexis F. Stimulus-responsive nanogels for drug delivery. Soft Matter. 2011;7(13):5908–5916.
27. Suhail M, Rosenholm JM, Minhas MU, et al. Nanogels as drug-delivery systems: a comprehensive overview. Ther Deliv. 2019;10(11):697–717.
28. Neamtu I, Rusu AG, Diaconu A, Nita LE, Chiriac AP. Basic concepts and recent advances in nanogels as carriers for medical applications. Drug Deliv. 2017;24(1):539–557.
29. Ghaywat SD, Mate PS, Parsutkar YM, Chandimeshram AD, Umekar MJ. Overview of nanogel and its applications. GSC Biol Pharm Sci. 2021;16(1):40–61.
30. Gugulothu S, Jatoth M, Rajitha E, et al. Formulation and development of nanogel containing green tea extract. Int J Res Publ Rev. 2024;8(5):700–710.
31. Patil TT, Shelake SS, Chougule NB. Formulation and evaluation of nanogel from benzocaine for analgesic activity. Int J Res Publ Rev. 2024;8(5):616–626.
32. Sangeetha S, Venkatesh S, Chandra S, Senthil Kumar S. Formulation and evaluation of baclofen nanogel using a synthetic polymer. Int J Pharm Anal Res. 2024;13(4):663–672.
33. Aparna C, Manisha B, Kalva S. Formulation and evaluation of etoricoxib nanogel. Int J Pharm Sci Res. 2023;78(1):113–118.
34. Bedse A, Nikam A, Kulkarni A, Potnis V, Dhamane S. Development and characterization of topical

microemulsion of dapsone. Int J Pharm Sci Nanotechnol. 2023;15(1):5805–5812.

35. Tanushree C, Rajesh V, Jaya S, Pankaj S. Full factorial design for optimization of clindamycin phosphate-loaded nanogel. Int J Pharm Pharm Res. 2022;24:160–171.
36. Saraogi GK, Tholiya S, Mishra Y, et al. Formulation development and evaluation of pravastatin-loaded nanogel for hyperlipidemia management. Gels. 2022;8(2):81.
37. Alam MS, Algahtani MS, Ahmad J, et al. Formulation design and evaluation of aceclofenac nanogel for topical application. Ther Deliv. 2020;11(12):767–778.
38. Oktay AN, Celebi N, Ilbasmis Tamer S, Kaplanoglu GT. Cyclodextrin-based nanogel of flurbiprofen for dermal application. J Drug Deliv Sci Technol. 2023;79:104012.
39. Hamzah ML. Formulation and evaluation of flurbiprofen nanogel. Res J Pharm Technol. 2020;13(11):5183–5188.
40. Manjunath SN, Yogananda R, Nagaraja TS. Preparation and characterization of a nanogel drug delivery system containing clotrimazole. Indo Am J Pharm Res. 2020;10(7).
41. Chopade S, Khabade S, Patil A, Powar S. Formulation development and evaluation of the anti-inflammatory potential of topical tenoxicam nanogel. Int J Pharm Sci Res. 2019;10(8):1000–1006.
42. Ahmad J, Gautam A, Komath S, et al. Topical nano-emulgel for skin disorders: formulation approach and characterization. Recent Pat Anti-Infect Drug Discov. 2019;14(1):36–48.
43. Avasatthi V, Pawar H, Dora CP, et al. A novel nanogel formulation of methotrexate for topical treatment of psoriasis. Pharm Dev Technol. 2016;21(5):554–562.
44. Yao Y, Xia M, Wang H, et al. Preparation and evaluation of chitosan-based nanogels/gels for oral delivery of myricetin. Eur J Pharm Sci. 2016;91:144–153.
45. Nandi I, Bari M, Joshi H. Study of isopropyl myristate microemulsion systems containing cyclodextrins to improve the solubility of two model hydrophobic drugs. AAPS PharmSciTech. 2003;4(1):10.